

DFT and TD-DFT studies on a schiff base containing phenylalanine derived from curcumin

Ping Deng^{a,b}, Hai-Dong Zhang^c, Jun-Hao Jiang^{a,b}, and Qi-Hua Jiang^{a,b,*}

^aSchool of Pharmacy, Chongqing Medical University, Chongqing 400016, China

^bEngineering Research Center of Drug, Chongqing Medical University, Chongqing 400016, China

^cEngineering Research Centre for Waste Oil Recovery Technology and Equipment, Ministry of Education, Laboratory of Applied Catalysis, Chongqing Technology and Business University, Chongqing 400067, China

Received 19 August 2010; Accepted (in revised version) 20 September 2010

Published Online 17 January 2011

Abstract. The structure of a schiff base containing phenylalanine derived from curcumin has been studied by computational simulations using density functional theory (DFT) and time-dependent density functional theory (TD-DFT) at B3LYP/6-311G** level. According to the theoretical calculations of three tautomers, enolic tautomer (*A*), enamine tautomer (*B*) and ketonic tautomer (*C*), of the schiff base molecular, the geometry, relative stability, charge density population and UV-Vis characteristics of every tautomer are investigated. The calculation results demonstrate that the enamine tautomer (*B*) is the most stable one and the stability of tautomers decreases in the sequence: $B > A > C$. The λ_{max} of each tautomer mainly originates from the $\pi - \pi^*$ electronic transition, involving the intramolecular charge transfer. The intramolecular proton transfer caused by electron transitions can result in the interconversion of *A* and *B* with a low energy barrier. Water can make the UV-Vis spectra of *A* and *B* exhibit remarkable red shift, increasing oscillator strength and absorption intensity. On the contrary, water can make *C* demonstrate a spectrum without shift, decreasing oscillator strength and absorption intensity.

PACS: 31.15.E

Key words: curcumin derivative, schiff base, phenylalanine, density functional theory (DFT)

1 Introduction

Curcumin, a natural yellow pigment in *Curcuma longa L.*, is attractive for its biological activity including anti-inflammatory, antioxidant and antitumor properties. Curcumin can change the redox property of cell and thus adjust the anti-inflammatory activity [1] and inhibit or

*Corresponding author. *Email address:* quantum_chemistry@126.com (Q. H. Jiang)

promote apoptosis [2], and inhibit capillary hyperplasia [3]. In addition, Curcumin has been found to be effective in treating the squamous cell carcinoma of head and neck, melanoma, sarcoma, leukemia, lymphoma, and the cancers of colon, breast, nervous system, lung, pancreas and ovarian [4–11]. For its low molecular weight, hypotoxicity, and definite biological activity, curcumin is considered as one potential ideal anti-cancer drug in chemotherapy. Unfortunately, its poor water solubility and inadequate absorption in vivo result in low bioavailability and greatly limit its clinical application. The structural modification of curcumin molecular, in order to increase its anti-tumor activity and water solubility while retaining its hypotoxicity, is hot in this field [12]. Amino acid schiff bases and their derivatives have attracted great attention because of their good biological activity and bio-solubility [13]. Seven 5-fluorouracil derivatives containing schiff bases with certain anti-tumor activity had been synthesized by Shi *et al.* [14].

As amino acid schiff bases have good biocompatibility with the carboxyl groups which can form salts to improve their water solubility, we design a schiff base containing phenylalanine derived from curcumin (Fig. 1). In vivo, this compound can hydrolyze and decompose into curcumin and phenylalanine. Then it may play the pharmacological role of curcumin. Furthermore, the designed compound contains a carboxyl group and then can be transformed into a water-soluble salt with good water solubility and bioavailability.

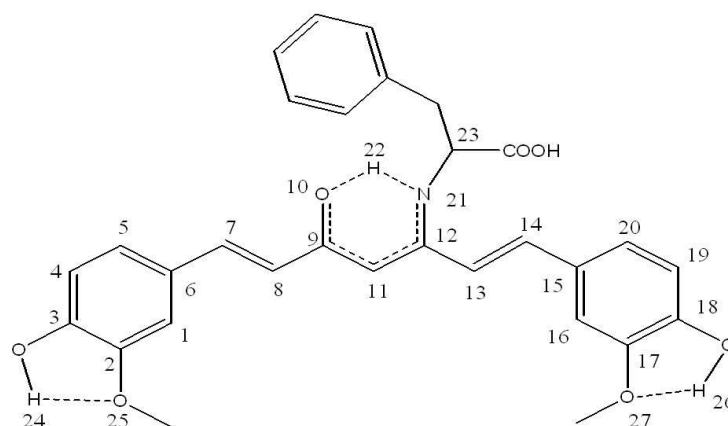


Figure 1: Schematic diagram and atomic numbers of the designed schiff base containing phenylalanine derived from curcumin.

Curcumin molecular possesses two isomers. One is di-ketonic while another is keto-enolic [15]. The designed schiff base may also possess isomers. In this work, we carry out theoretical studies on the geometry, relative stability, charge density population and UV-Vis characteristics of the designed schiff base to provide valuable reference for the synthesis. As widely used in the theoretical studies on molecular electronic structure and spectral properties, density functional theory (DFT) and time-dependent density functional theory (TD-DFT) [16] are used in the simulations in this work to do high-level computational analysis of the designed compound.

2 Computational details

All calculations in this work were performed using Gaussian 03 package [18]. In order to obtain relatively accurate results, DFT calculations were carried out with Becke's three-parameter nonlocal exchange functional [19] and Lee, Yang, and Parr nonlocal correlation functional (B3LYP) at 6-311G** level [15]. The designed compound possesses three tautomers: enolic tautomer (*A*), enamine tautomer (*B*) and ketonic tautomer (*C*). The geometry of every involved tautomer was fully optimized at the above level. On the basis of calculations, the relative stability, charge density population and intramolecular proton transfer of designed compound have been discussed in details. Using TD-DFT method, the UV-Vis characteristics of each tautomer were investigated at the same level. The solvent effect in water was estimated with Polarized continuum model (PCM) [17] to approach the real conditions. The electronic charge densities at the bond critical point (BCP) and charges of some critical atoms were calculated with AIM 2000 package [20] to get a deep insight into the nature of hydrogen-bonding interaction and intramolecular proton transfer.

3 Results and discussion

3.1 Geometry characteristics

In order to obtain reliable and stable structures, vibration frequencies were calculated for all optimized structures of three tautomers. No imaginary frequency for each one is found, indicating the authenticity of calculations. The configurations of tautomers *A*, *B* and *C* in vacuum are illustrated in Fig. 2. Part of the data of bond length and charge density at BCP are listed in Table 1.

Table 1: Part of the data of bond length (in nm) and charge density at BCP (in a.u.).

Medium	H24-O25		H26-O27		N21-C12		N21-H22		O10-H22		O10-C9		
	Bond length	$\rho(r)$											
<i>A</i>	vacuum	0.2076	0.0211	0.2077	0.0210	0.1307	0.3556	0.1648	0.0624	0.1013	0.3089	0.1330	0.3122
	water	0.2079	0.0211	0.2079	0.0211	0.1309	0.3542	0.1607	0.0689	0.1022	0.3077	0.1336	0.3096
<i>B</i>	vacuum	0.2074	0.0212	0.2078	0.0210	0.1361	0.3160	0.1024	0.3279	0.1849	0.0352	0.1250	0.3758
	water	0.2078	0.0211	0.2080	0.0211	0.1358	0.3176	0.1024	0.3271	0.1849	0.0351	0.1258	0.3709
<i>C</i>	vacuum	0.2073	0.0212	0.2074	0.0212	0.1283	0.3731					0.1218	0.4021
	water	0.2075	0.0213	0.2078	0.0211	0.1282	0.3738					0.1224	0.3972

The skeleton structures of *A* and *B* are "T" shape because of the $\pi-\pi$ conjugation in moleculars. The skeleton structure of *C* possesses two conjugated system divided into by C11 atom and looks like "Y" shape. In vacuum, all tautomers show two weak intramolecular hydrogen bonds involving 18 or 3-phenolic hydrogen atom and 17 or 2-methoxylic oxygen atom. The bond length of the hydrogen bonds H24—O25 and H26—O27 varies from 0.2074

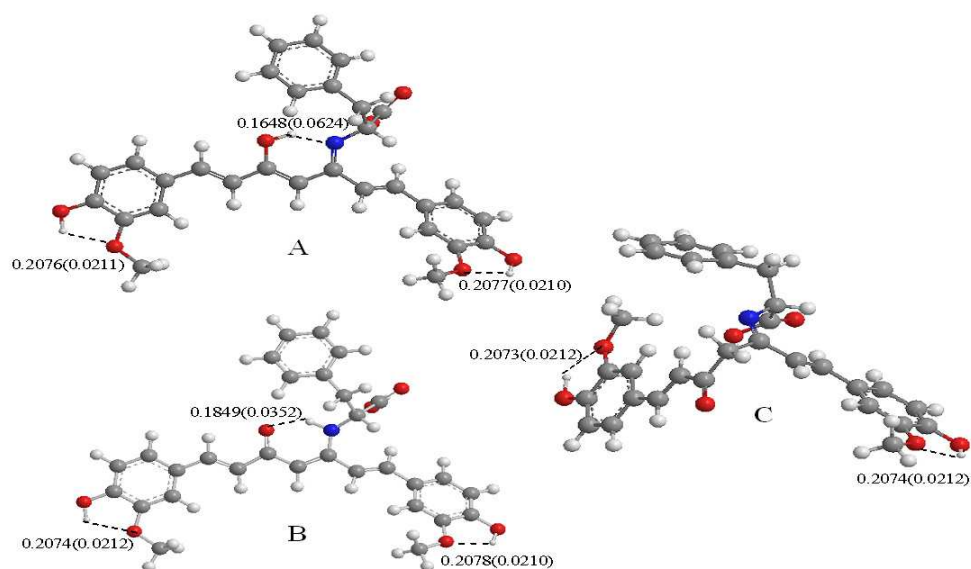


Figure 2: Hydrogen bonding structures for three tautomers in vacuum: bond length in nm, charge density at BCP in a.u..

to 0.2078 nm. The electron density at BCP of these weak bonds are about 0.0211 a.u.. In addition, two strong intramolecular hydrogen bonds are found, involving H22 and N21 in *A* while involving H22 and O10 in *B*. The length of bond N21—H22 in *A* is 0.1648 nm while its charge density at BCP is 0.0625 a.u.. Koch and Popelier proposed the criteria of hydrogen-bonding: the value of $\rho(r)$ at BCP of bond H-Y lies within the range of 0.002~0.040 a.u. [21] Thus, the hydrogen bond N21···H22 in *A* is more stronger than the traditional hydrogen bond. In *B*, the length and the charge density at BCP of bond H22—O10 is 0.1849 nm and 0.0352 a.u.. The value of $\rho(r)$ is in the range of 0.002~0.040 a.u., indicating that bond H22—O10 is a traditional hydrogen bond. These results also reflect the interconversion between *A* and *B* by intramolecular proton transfer. In vacuum, the net distance of such transfer is 0.0624 nm for the conversion from *A* to *B* or 0.0837 nm for the conversion from *B* to *A*.

The length (0.1607 nm) of bond N21···H22 of *A* in water is shorter than the value in vacuum, indicating a stronger O-H···N hydrogen bond. However, the length (0.1849 nm) of bond H22···O10 of *B* in water is similar to the value in vacuum, showing less impact of water on N-H···O hydrogen bond. This may be due to the strong interactions between H₂O molecules and O10 atom. The net distance of intramolecular proton transfer in water is 0.0583 nm for the conversion from *A* to *B*, or 0.0827 nm for the conversion from *B* to *A*. The shorter net distance of intramolecular proton transfer in water reflects that the intramolecular proton transfer is more achievable in water than in vacuum.

The thermodynamics parameters, E , U , H and G , of each tautomer were calculated at B3LYP/6-311G** level. For comparison, the relative values, ΔE , ΔU , ΔH and ΔG are collected and shown with E , U , H and G in Table 2. The calculation results confirm that the enamine

tautomer is the most stable one and the stability of tautomers decreases in the sequence: $B > A > C$, which is in good agreement to the studies by Benassi *et al.* [15]. Mezey *et al.* [22] reported that the tautomers can coexist in the same equilibrium system, even if the energy difference between two tautomers is about 40 kJ/mol. According to our results, the three tautomers would coexist in an equilibrium system but the main form should be enamine tautomer (*B*).

Table 2: Thermodynamics parameters of each tautomer calculated by DFT.

medium	<i>E</i> (a.u.)	<i>U</i> (a.u.)	<i>H</i> (a.u.)	<i>G</i> (a.u.)	ΔE (kJ/mol)	ΔU (kJ/mol)	ΔH (kJ/mol)	ΔG (kJ/mol)	
A	vacuum	-1742.3905	-1741.8211	-1741.8201	-1741.9316	25.98	22.71	22.71	25.38
	H ₂ O	-1742.4149	-1741.8465	-1741.8456	-1741.9573	31.01	27.28	27.28	30.57
B	vacuum	-1742.4004	-1741.8297	-1741.8288	-1741.9412	0.00	0.00	0.00	0.00
	H ₂ O	-1742.4267	-1741.8569	-1741.8560	-1741.9689	0.00	0.00	0.00	0.00
C	vacuum	-1742.3833	-1741.8136	-1741.8126	-1741.9254	44.91	42.48	42.48	41.57
	H ₂ O	-1742.4082	-1741.8395	-1741.8386	-1741.9525	48.68	45.67	45.67	43.21

3.2 UV-Vis spectroscopy

To fully understand the designed compound, we also investigated the maximum absorption wavelength (λ_{max}), oscillator strength (f), excitation energy (E_{ex}) and composition of electronic transition for each tautomer using TD-DFT method at B3LYP/6-311G** level and list data in Table 3. Water causes a red shift of the λ_{max} for *A* and *B* with higher oscillator strength and absorption intensity. On the contrary, the effect of water on the λ_{max} of *C* is little with lower oscillator strength and absorption intensity. The λ_{max} of *A* and *B* are mainly determined by the $\pi-\pi^*$ electronic transition of H \rightarrow L either in vacuum or in water. In vacuum, the λ_{max} of *A* is 405 nm with 0.89 for f . The λ_{max} of *A* shifts to 416 nm in water while the f of *A* increases to 1.23. The λ_{max} and f of *B* changes in same way as that for *A*. Notably, the λ_{max} of *C* is mainly determined by the $\pi-\pi^*$ electronic transitions of H \rightarrow L+1 both in vacuum and in water. The solvent effect on absorption spectra of *C* is negligible. The electron density distribution of molecular frontier orbitals shows that all the electronic transitions involve the intramolecular charge transfer.

3.3 Charge density population

A hydrogen bond, a weak chemical bonding with bonding energy usually at 5 to 30 kJ/mol, is the attractive interaction of a hydrogen atom with an electronegative atom [23] like nitrogen, oxygen or fluorine. Electronic charge density and milliken population of the active atoms in *A*, *B* and *C* are shown in Table 4. Zhang *et al.* confirmed that bigger charge density changes of the active hydrogen atom will result in higher energy barrier in proton transfer processes [24]. The small charge density difference for H22 atom of *A* and *B* indicates low energy barrier for the

intramolecular proton transfer. Such transfer can take place easily and thus results in the easy interconversion of *A* and *B*. The charge density of H22 atom in *C* is much lower than that in *A* or *B*. Reasonably, a relatively higher energy barrier for proton transfer can be found for *C*. The charge density of H-bond donor atom (O10) is increasing in the proton transfer process from *A* to *B* while the charge density of H-bond acceptor atom (N21) is decreasing. Reverse conversion of *B* to *A* shows similar characteristics. This transfer involving proton donor and proton acceptor may be caused by the π electron transitions in conjugated system, which is consistent with the typical intramolecular proton transfer reaction [25].

Table 3: Electronic absorption data calculated by TD-B3LYP/6-311G**.

	Medium	λ_{max} (nm)	E_{ex} (eV)	f	Configurations ^a
<i>A</i>	vacuum	405	3.06	0.89	H→L (95%)
	H ₂ O	416	2.98	1.23	H→L (95%)
<i>B</i>	vacuum	419	2.96	1.01	H→L (100%)
	H ₂ O	431	2.88	1.33	H→L (100%)
<i>C</i>	vacuum	332	3.74	0.627	H→L+1 (72%)
	H ₂ O	330	3.76	0.456	H→L+1 (72%)

^a H, L and L+1 represent HOMO, LUMO and LUMO+1 respectively.

Table 4: Charge population for the active atoms.

	Medium	Electronic charge density by AIM200 (a.u.)			Mulliken charge population (<i>e</i>)		
		O10	H22	N21	O10	H22	N21
<i>A</i>	vacuum	-1.058	0.622	-0.971	-0.352	0.286	0.480
	H ₂ O	-1.054	0.622	-0.964	-0.383	0.281	-0.491
<i>B</i>	vacuum	-1.100	0.475	-0.956	-0.437	0.265	-0.394
	H ₂ O	-1.119	0.497	-0.959	-0.473	0.257	-0.404
<i>C</i>	vacuum	-1.038	0.033	-0.966	-0.319	0.147	-0.288
	H ₂ O	-1.051	0.035	-0.941	-0.369	0.153	-0.304

4 Conclusions

According to the results of theoretical calculations, we demonstrate that the designed compound derived from curcumin possesses three possible stable tautomers: enolic tautomer (*A*), enamine tautomer (*B*) and ketonic tautomer (*C*). *B* is the most stable one. The interconversion of *A* and *B* can be easily achieved by intramolecular proton transfer. In vacuum, the net distance of transfer is 0.0624 nm for the conversion from *A* to *B* or 0.0837 nm for the conversion from *B* to *A*. The corresponding datum in water is 0.0583 nm or 0.0827 nm. The reduction of net distance between *A* and *B* in water indicates that the intramolecular proton

transfer can take place more easily between *A* and *B* in water than in vacuum. The electronic charge density and milliken population at B3LYP/6-311G** level of the active atoms in this designed compound furtherly confirm that the intramolecular proton transfer can take place easily between *A* and *B* with low energy barriers and the charge density of H-bond donor atom (O10) is increasing while the charge density of H-bond acceptor atom (N21) decreasing during the proton transfer process.

The λ_{max} of the adsorption spectrum of each tautomer is mainly determined by $\pi-\pi^*$ electronic transition while intramolecular charge transfer is also involved. Water can cause red shift of the λ_{max} for *A* and *B* with higher oscillator strength and absorption intensity. On the contrary, the effect of water on the λ_{max} for *C* is little with lower oscillator strength and absorption intensity.

Acknowledgments. The authors thank the support from the Ministry of Science and Technology of the People's Republic of China under Grant No. 2009GJF10005.

References

- [1] S. K. Sandur, H. Ichikawa, M. Pandey, *et al.*, Free Radical. Biol. Med. 43 (2007) 568.
- [2] A. Kunwar, S. K. Sandur, M. Krishna, *et al.*, Eur. J. Pharmacol. 611 (2009) 8.
- [3] B. B. Aggarwal, A. Kumar, and A. C. Bharti, Anticancer Res. 23 (2003) 363.
- [4] P. Anand, C. Sundaram, S. Jhurani, *et al.*, Cancer Lett. 267 (2008) 133.
- [5] A. B. Kunnumakkara, P. Anand, and B. B. Aggarwal, Cancer Lett. 269 (2008) 199.
- [6] J. J. Johnson and H. Mukhtar, Cancer Lett. 255 (2007) 170.
- [7] P. G. Radhakrishna, A. S. Srivastava, T. I. Hassanein, *et al.*, Cancer Lett. 208 (2004) 163.
- [8] S. S. Lin, K. C. Lai, S. C. Hsu, *et al.*, Cancer Lett. 285 (2009) 127.
- [9] W. Glienke, L. Maute, J. Wicht, *et al.*, Eur. J. Cancer 45 (2009) 874.
- [10] M. X. Shi, Q. F. Cai, L. Y. Yao, *et al.*, Cell Biol. Int. 30 (2006) 221.
- [11] M. Montopoli, E. Ragazzi, G. Frolidi, *et al.*, Cell Prolif. 42 (2009) 195.
- [12] G. Liang, J. L. Tian, L. L. Shao, *et al.*, Chemistry 71 (2008) 110.
- [13] P. Hu, K. Q. Zhao, H. B. Xu, and L. F. Zhang, Acta Chim. Sin. 60 (2002) 1682.
- [14] D. Q. Shi, Q. Chen, and Z. H. Li, Chinese J. Org. Chem. 25 (2005) 549.
- [15] R. Benassi, E. Ferrari, S. Lazzari, *et al.*, Mol. Struct. 892 (2008) 168.
- [16] C. Lee, W. Yang, and R. G. Parr, Phys. Rev. B 37 (1988) 785.
- [17] M. Cossi, V. Barone, R. Cammi, *et al.*, Chem. Phys. Lett. 255 (1996) 327.
- [18] M. J. Frisch, G. W. Trucks, H. B. Schlegel, *et al.*, Gaussian 03, Version D01 (Gaussian Ins., Wallingford CT, 2005).
- [19] A. D. Becke, J. Chem. Phys. 98 (1993) 5648.
- [20] G. W. Wang, M. H. Chen, and M. F. Zhou, Chem. Phys. Lett. 412 (2005) 46.
- [21] U. Kock and P. L. A. Popelier, J. Phys. Chem. 99 (1995) 9747.
- [22] P. G. Mezey, J. J. Ladik, and M. Bary, Theor. Chim. Acta. 54 (1980) 251.
- [23] X. F. Xu, F. Gao, H. R. Li, and S. T. Zhang, Acta. Phys. Chim. Sin. 26 (2010) 131.
- [24] H. Y. Zhang, J. Photochem. Photobiol. A 126 (1999) 27.
- [25] D. Z. Chen, D. P. Wang, H. Y. Zhang, *et al.*, Chem. Phys. Lett. 353 (2002) 119.